International Journal of Mass Spectrometry 379 (2015) 26–32

Contents lists available at ScienceDirect

International Journal of Mass Spectrometry

journal homepage: www.elsevier.com/locate/ijms

Insights into the fragmentation pathways of gas-phase protonated sulfoserine

Amanda L. Patrick[a], Corey N. Stedwell[a], Baptiste Schindler[b,c,d], Isabelle Compagnon[b,c,d,e], Giel Berden[f], Jos Oomens[f,g], Nicolas C. Polfer[a,*]

[a] Department of Chemistry, University of Florida, P.O. Box 117200, Gainesville, FL 32611, USA
[b] Université de Lyon, F-69622 Lyon, France
[c] Université Lyon 1, Villeurbanne, France
[d] Institut Lumière Matière, UMR5306 Université Lyon 1-CNRS, Université de Lyon, 69622 Villeurbanne Cedex, France
[e] Institut Universitaire de France IUF, 103 Blvd St. Michel, 75005 Paris, France
[f] Radboud University Nijmegen, Institute for Molecules and Materials, FELIX Laboratory, Toernooiveld 7, 6525ED Nijmegen, The Netherlands
[g] van 't Hoff Institute for Molecular Sciences, University of Amsterdam, Science Park 904, 1098XH Amsterdam, The Netherlands

ARTICLE INFO

Article history:
Received 3 October 2014
Received in revised form 4 December 2014
Accepted 5 December 2014
Available online 23 December 2014

Keywords:
Post-translational modifications
Sulfation
IRMPD spectroscopy

ABSTRACT

The fragmentation chemistry of protonated sulfoserine was probed using a combination of collision-induced dissociation (CID) mass spectrometry, infrared multiple photon dissociation (IRMPD) spectroscopy, and density functional theory (DFT) calculations. The IRMPD spectra of the dominant fragment ions at *m*/*z* 106 and 88 (*i.e.*, loss of SO_3 and H_2SO_4) were obtained and used to determine the corresponding structures. By comparison to a synthetic standard and calculations, it was determined that the *m*/*z* 106 ion is structurally identical to protonated serine. The *m*/*z* 88 fragment ion was assigned an aziridine structure based on a comparison to theory, analogous to the structure previously proposed by others for phosphoric acid loss from phosphoserine. This work provides the first spectroscopic insights into the dissociation pathways of a sulfated amino acid, laying the groundwork for future studies on related amino acids and peptides with this important, labile post-translational modification.
© 2014 Elsevier B.V. All rights reserved.

1. Introduction

Peptide sulfation at tyrosine is a relatively common post-translational modification (PTM), with known roles in various biological processes, including the binding of blood coagulation proteins [1–3] and hormone recognition by receptors [4]. Sulfation of serine and threonine was only first reported in 2004 [5]. This novel modification was detected in proteins from systems ranging from the unicellular malaria parasite, *Plasmodium falciparum*, to humans, which suggests that this too is a key biological modification warranting further study. Furthermore, whilst tyrosine sulfation is slowly beginning to be recognized as a worthwhile analytical and mass spectrometric challenge, the behavior of sulfothreonine- and sulfoserine-containing peptides under various mass spectrometric conditions has gained significantly less attention. Thus, it is useful to begin forming a foundational understanding of the gas-phase fragmentation chemistry of these species, beginning here with a model system, protonated sulfoserine.

Despite the biological significance of peptide sulfation, sulfoproteomics [6] has thus far been less successful than phosphoproteomics [7–9] at gaining recognition as a routine sub-field of proteomics. Due, for example, to the acid and gas-phase lability of the sulfate group, sulfopeptides present distinctive challenges for the mass spectrometry community. Nonetheless, recently some significant strides have been made toward the analysis of sulfotyrosine-containing peptides by mass spectrometric methods. Differentiating sulfotyrosine-containing peptides from phosphotyrosine-containing peptides has been demonstrated by use of high-resolution mass spectrometry [10] and resonant infrared photodissociation spectroscopy [11]. Furthermore, attempts to sequence sulfopeptides have been pursued, with some success, by employing radical dissociation chemistry, such as negative ion electron capture dissociation (niECD) [12], electron transfer/capture dissociation (ETD/ECD) [13], and ultraviolet photodissociation (UVPD) [14]. Alternative approaches have included chemical modification of free tyrosine residues, followed by quantitative removal of sulfate groups from sulfated tyrosine residues, to allow for the indirect determination of sulfation

* Corresponding author. Tel.: +1 352 392 0492; fax: +1 352 392 0872.
E-mail address: polfer@chem.ufl.edu (N.C. Polfer).

http://dx.doi.org/10.1016/j.ijms.2014.12.001
1387-3806/© 2014 Elsevier B.V. All rights reserved.

site(s) through collision-induced dissociation (CID) sequencing [15].

A key aspect of understanding gas-phase fragmentation pathways involves elucidating the structure of the resulting product ions. One of the most powerful techniques for this purpose is infrared multiple photon dissociation (IRMPD) spectroscopy [16,17]. Since infrared photodissociation is only induced when the impinging photon is of a resonant energy with a vibrational mode of the analyte, by recording photofragmentation as a function of photon energy, an IRMPD spectrum, analogous to a more traditional absorption IR spectrum, can be constructed. IRMPD spectroscopy thus serves as a direct structural probe of gas-phase ions and can be used for structural elucidation of said ions, especially when combined with theoretical infrared (IR) frequency calculations and/or comparison to experimental spectra of synthetic standards. This technique has proven successful in many areas, including the study of PTMs [18–21] and of the fragmentation chemistry of peptides [22–25] and remains promising for many additional future applications.

As phosphoproteomics has outpaced sulfoproteomics, studies on the fragmentation pathways of phosphopeptides upon collisional activation [20,26–28] have likewise been more prevalent than comparable studies for sulfopeptides, which are essentially nonexistent thus far. The present study aims to begin closing this gap and shed light on the CID fragmentation patterns of protonated sulfoserine. This is achieved through the combination of various approaches, including IRMPD spectroscopy, CID tandem mass spectrometry, and DFT calculations.

2. Methods

2.1. Experimental methods

Sulfoserine and serine were obtained from Bachem (Bubendorf, Switzerland). Solutions were prepared at concentrations of 100–1000 μM in either 70/30 or 50/50 methanol/water with either 0.1 or 1% acetic or formic acid added to obtain optimal mass spectrometric signal for high quality IRMPD spectra.

To provide an in-depth understanding of the structure and fragmentation pathways of the protonated sulfoserine ion, several complementary mass spectrometry and ion spectroscopy experiments were conducted. Thus, three instrumental setups were used:

(1) IRMPD spectra in the fingerprint region were recorded using a Fourier transform ion cyclotron resonance (FTICR) mass spectrometer coupled to the beamline of the Free Electron Laser for Infrared eXperiments (FELIX) [29,30]. Briefly, precursor ions were generated by electrospray ionization (ESI) using a Micromass Z-Spray source, trapped in the ICR cell, and mass isolated by a stored waveform inverse Fourier transform (SWIFT) excitation pulse [31]. Fragment ions were generated *via* fixed-wavelength irradiation with a CO_2 laser at 10.6 μm, and subsequently mass isolated before analysis. Finally, the ions of interest were irradiated with the tunable output from FELIX. The corresponding (power-corrected) photodissociation yield was calculated by monitoring the abundances of the parent and precursor ions. Irradiation times were chosen to induce sufficient dissociation for each ion (*e.g.*, 2–4 s), with 10 macropulses per second. Typical macropulse energies were ~40 mJ.

(2) IRMPD spectra in the NH/OH stretching region and CID experiments were measured using a Thermo Finnigan LCQ 3D ion trap with an ESI source. This mass spectrometer was modified to allow for the entrance of the laser beam from a YAG-pumped tunable IR optical parametric oscillator/amplifier (OPO/A) (LaserVision), which was focused on the ion cloud. This OPO operates at a repetition rate of 10 Hz with an average pulse energy of approximately 15 mJ (which corresponds to a radiation energy of 0.15 J per second). This set up has been described previously [32]. The mass-isolated protonated sulfoserine precursor was subjected to CID to form the fragment ion of interest, which was then mass isolated before irradiation with the output of the OPO. Typical irradiation times were 800–1900 ms, depending on the analyte. By recording fragmentation as a function of irradiation wavelength, IRMPD spectra were obtained.

(3) To demonstrate inter-setup reproducibility of results, the IRMPD spectrum of the *m*/*z* 88 fragment ion was also recorded using a custom-built hybrid mass spectrometer for IRMPD spectroscopy, described elsewhere [33]. In short, protonated ions were generated by ESI using a custom source, fragmented in-source *via* nozzle-skimmer CID, mass selected by a quadrupole mass filter (QMF), and trapped in a reduced-pressure quadrupole ion trap (QIT). Here, the ions were irradiated (1 s irradiation time, in this experiment) with a focused IR beam from a tunable optical parametric oscillator/amplifier (OPO/A) (LINOS Photonics OS4000) to induce photodissociation. This OPO generates continuous wave (cw) output with powers generally between 20 and 50 mW (which corresponds to a radiation energy of 0.02–0.05 J per second), depending on the wavelength. Due to variable power from one wavelength to the next, each data point was power corrected to account for such fluctuations.

For all IRMPD spectra, the linear IRMPD yield was calculated (see Eq. (1)) and plotted as a function of photon energy, given in wavenumber (cm^{-1}).

$$\text{IRMPD yield} = \frac{\sum(\text{photofragments})}{\sum(\text{photofragments} + \text{precursor})} \quad (1)$$

2.2. Computational methods

Chemical structures and conformations of protonated sulfoserine, protonated serine, and three potential isomers of *m*/*z* 88 were generated using Gabedit [34]. Energy optimization and IR frequencies were then calculated using Gaussian 09 [35] for each unique conformer using density functional theory at the B3LYP level of theory with the aug-cc-pVTZ basis set. This basis set was chosen because it has been previously employed for sulfur-containing systems [36]. Infrared spectra and molecular motions were visualized in Gabedit [34] and/or Avogadro [37]. Scaling factors of 0.973 for the region 550–1900 cm^{-1} and 0.960 for 3200–3700 cm^{-1} were applied, consistent with previous reports [20]. Computed line spectra were convoluted with a 10 cm^{-1} or 30 cm^{-1} (for the NH/OH-stretching region and mid-IR region, respectively) full-width-at-half-maximum Gaussian line shape for ease of comparison with experimental spectra.

3. Results and discussion

3.1. CID of protonated sulfoserine

The mass spectrum of protonated sulfoserine is shown in the upper panel of Fig. 1; the lower panel shows the resulting MS^2 spectrum after CID. Protonated sulfoserine was observed to produce four main fragment ions at *m*/*z* 140, 129, 106, and 88, with the most intense fragments arising from loss of the sulfate modification as either SO_3 or H_2SO_4 (*i.e.*, −80 and −98 amu, respectively). As the corresponding HPO_3 and H_3PO_4 loss ions are of interest to the phosphoproteomics community, these sulfate-loss fragment ions are of potential sulfoproteomic interest and, thus, will each be analyzed

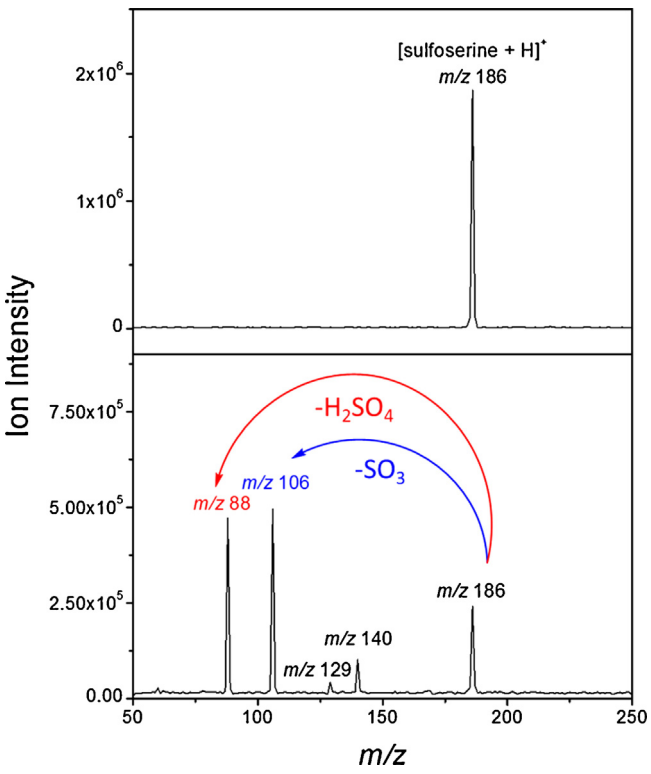

Fig. 1. The MS of the mass isolated precursor ion, protonated sulfoserine, is shown in the top panel. The bottom panel illustrates the mass spectrum after 60 ms of CID at 20% normalized collision energy. Fragment ions are observed at *m*/*z* 140, 129, 106, and 88. The fragment ions at 106 and 88 result from loss of the PTM as SO_3 (*m*/*z* 106, blue) and H_2SO_4 (*m*/*z* 88, red).

by IRMPD spectroscopy in turn in the following sections of this paper. Note that for the sake of completeness, the IRMPD spectrum of protonated sulfoserine was also recorded and is shown in Fig. S1 of the supplementary data, but this is not a focus of this paper.

The *m*/*z* 106 ion corresponds to the mass of protonated serine and can be readily interpreted as a direct loss of SO_3. For the *m*/*z* 88 ion, on the other hand, either a direct loss of H_2SO_4 or a sequential loss of SO_3 followed by H_2O can be envisioned to explain the overall observed loss of 98 amu. To gain further insights as to which pathway dominates, the CID mass spectrum of serine was obtained and kinetic CID experiments were performed. The CID mass spectrum of protonated serine (shown in Fig. S2) shows that there are two main fragment ions, namely *m*/*z* 88 and *m*/*z* 60 (loss of H_2O and $H_2O + CO$, respectively), of which *m*/*z* 60 is dominant. This observation is consistent with those reported by others [38,39]. It is worth mentioning that in Fig. 1 there is only ~3% of the aforementioned *m*/*z* 60 fragment, which supports the hypothesis that the sequential fragmentation of *m*/*z* 106 (to *m*/*z* 88) is a lesser channel under these particular conditions.

Distinguishing between competitive fragmentation pathways and sequential processes can be achieved *via* kinetic studies, as proposed in, for example [38]. The breakdown graph for sulfoserine, measured as a function of the CID activation energy, is shown in Fig. 2. Fragmentation as a function of activation time is also presented in Fig. S3. It appears that the two main fragmentation pathways follow first-order kinetics, in agreement with competitive, rather than sequential, fragmentation. Also, it can be noted that the relative abundance of the *m*/*z* 88 ion increases with collisional energy, which is consistent with a higher activation energy to formation and a looser transition state for this pathway. In summary, while it is impossible to completely rule out the possibility of a sequential loss pathway being at play, the evidence presented

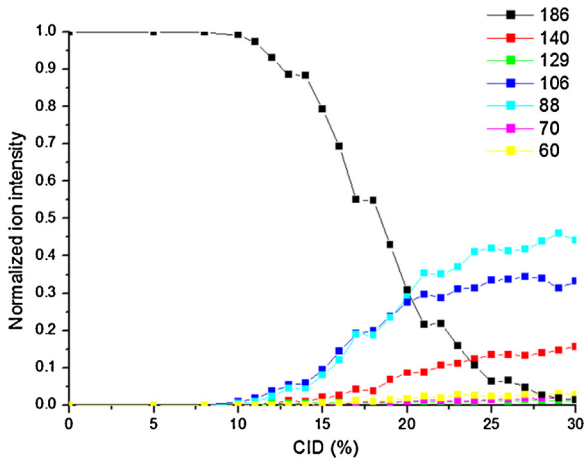

Fig. 2. The intensity of the precursor ion (*m*/*z* 186) and each fragment as a function of CID activation energy (25 ms activation time).

herein is all consistent with a direct loss of H_2SO_4 for the formation of the observed *m*/*z* 88 ion from protonated sulfoserine.

3.2. Structural elucidation

3.2.1. *m*/*z* 106 fragment ion

A hypothesized mechanism by which sulfoserine may lose SO_3 (80 amu) is presented in Scheme 1. This mechanism generates a fragment ion at *m*/*z* 106, which is structurally identical to protonated serine.

To test this hypothesis, the IRMPD spectrum of the *m*/*z* 106 fragment ion from sulfoserine was compared to both the experimental and theoretical spectra of protonated serine. The results of these measurements are presented in Fig. 3, showing the mid-IR and NH/OH-stretching regions. The experimental spectrum of the *m*/*z* 106 fragment ion is a nearly identical replica of that of the serine standard, with only very minor differences in the intensities of a few bands. It should also be noted that the theoretical IR spectrum of the lowest energy conformer of protonated serine provides a convincing match in both infrared regions. Structures and energies of the lowest-energy conformer of serine are presented in Fig. S4 and Table S1. Together, this provides conclusive evidence that the fragment ion at *m*/*z* 106 is indeed structurally analogous to protonated serine.

3.2.2. *m*/*z* 88 fragment ion

When considering the loss of 98 amu from sulfoserine, it is probable that the fragmentation mechanism might be similar to that of phosphoserine, except with the loss of H_2SO_4, rather than H_3PO_4. Previous studies have investigated the fragmentation mechanisms of phosphopeptides, by experimental and theoretical means [27,40]. More relevant here, the phosphoric acid loss fragment ion from phosphoserine has been identified as

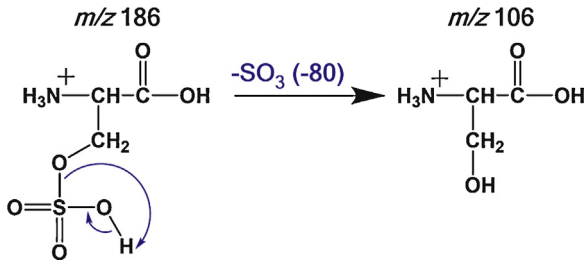

Scheme 1.

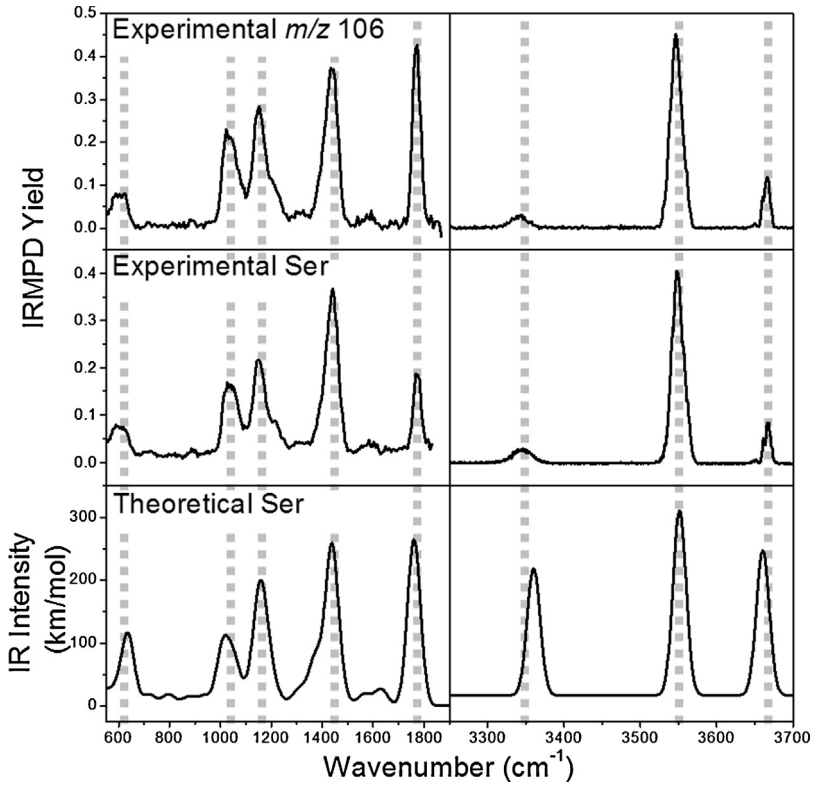

Fig. 3. IRMPD spectra of the *m*/*z* 106 fragment ion from sulfoserine (top) and of a serine standard (middle) compared to the theoretical IR spectrum of the lowest energy conformer of serine (bottom) in the regions of 550–1900 and 3200–3700 cm^{-1}.

2-carboxy-aziridine using traditional mass spectrometric methods (*e.g.*, deuterium labeling and MS^3) [28] and, more recently, by IRMPD spectroscopy [20]. Due to the similarities between the phosphate and sulfate modifications, one can propose various possible mechanisms (panel I of Scheme 2) for sulfuric acid loss from sulfoserine based on these previous studies. Pathway I-A represents a 1,2-*cis*-β-elimination of H_2SO_4, which generates 2-amino-propenoic acid. In pathway I-B, the protonated

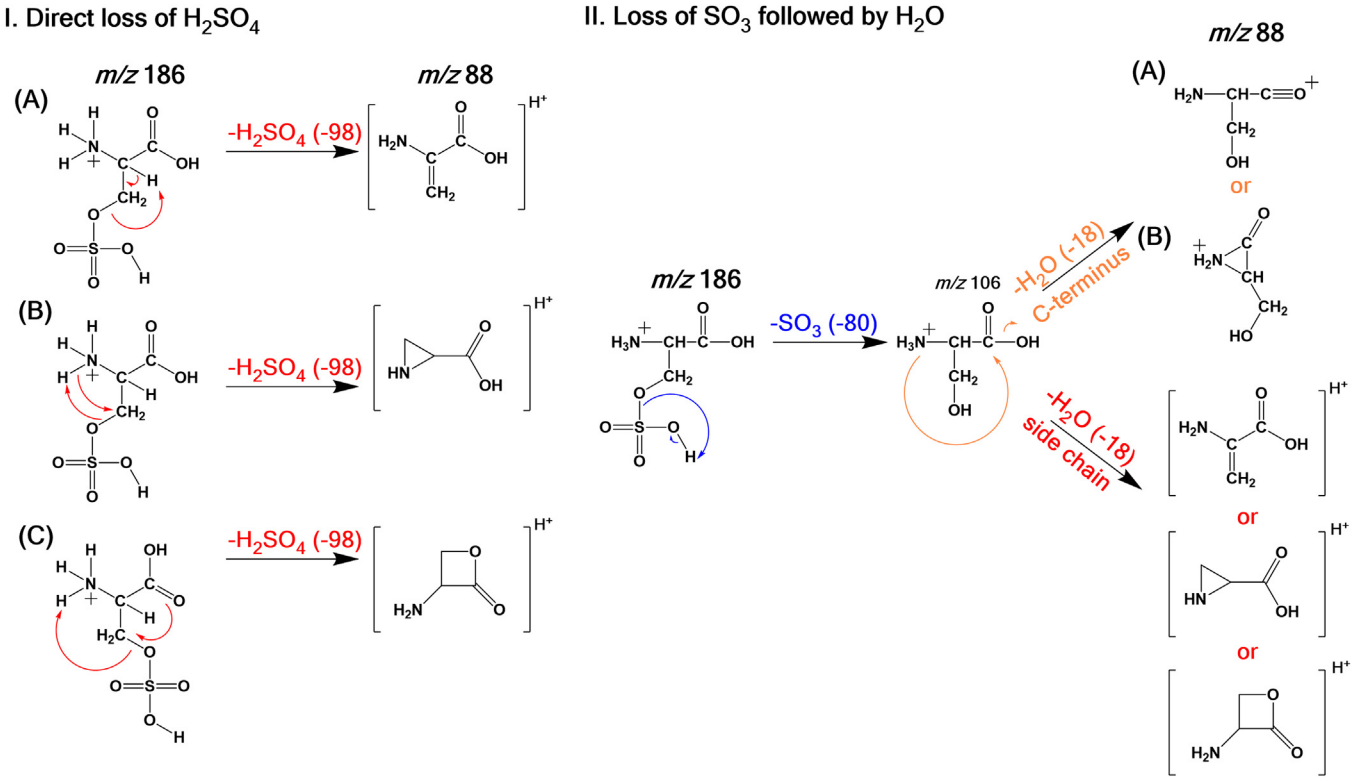

Scheme 2.

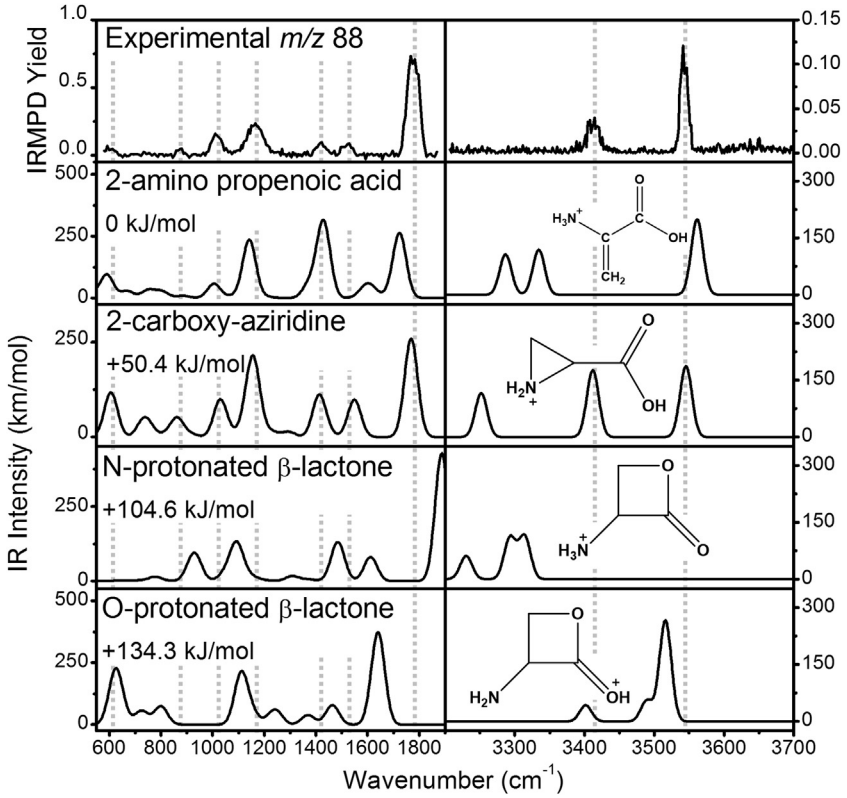

Fig. 4. The IRMPD spectrum of the *m*/*z* 88 fragment ion, in the regions of 550–1900 and 3200–3700 cm^{-1}, is given in the top panel. Calculated IR spectra for the lowest energy conformer of the different potential fragment ion isomers (2-amino propenoic acid, 2-carboxy-aziridine, O-protonated β-lactone, and N-protonated β-lactone) are then provided in the lower panels, as labeled, for comparison.

sulfoserine undergoes nucleophilic attack by the amino group on the β-carbon, which forms 2-carboxy-aziridine. Pathway I-C produces a β-lactone (which can be protonated at either the amine or the carbonyl) *via* a nucleophilic attack of the carbonyl oxygen of the C-terminus on the β-carbon. Structures and energies of each of the conformers found for the four candidate isomers of the *m*/*z* 88 ion are presented in Fig. S5 and Table S1. As mentioned in section 3.1, it is also possible to envision a sequential loss pathway in which loss of SO_3 is followed by loss of H_2O. Examples of such pathways are given in panel II of Scheme 2. Furthermore, in this case one must consider water loss from either the carboxylic acid (top half of panel II of Scheme 2) or from the hydroxyl side chain (lower half). Note that the hydroxyl side chain water losses could give rise to the same ion structures as expected from direct H_2SO_3 loss. If the water loss occurs from the carboxylic acid, it could occur *via* direct loss of H_2O to form an acylium ion (II-A) or through nucleophilic attack by the N-terminus on the carbonyl C to form a 3-membered ring (II-B). Acylium ions are generally not considered stable and would be expected to undergo spontaneous loss of CO [41] and previous studies of isotope-labeled protonated threonine have shown that side-chain water loss is favorable when water is lost by itself [42]. Here, we use IRMPD spectroscopy to determine the structure of the *m*/*z* 88 ion formed from the fragmentation of sulfoserine.

The experimental IRMPD spectra of the *m*/*z* 88 fragment ion from protonated sulfoserine are given in the top panel of Fig. 4. A key chemical insight from these spectra can be gleaned from the hydrogen stretching region. The observation of the signature carboxylic acid OH stretch (~3550 cm^{-1}), contrasted with the lack of a side-chain (alcohol) OH stretch (expected at ~3660 cm^{-1}, based on the protonated serine spectrum in Fig. 3), gives compelling evidence that loss of the C-terminal carboxylic acid OH is not observed. Such structures (*e.g.*, Scheme 2II-B) could thus be ignored in the computational search. All calculated fragment ion structures for the *m*/*z* 88 ion, and various minima conformers, are depicted in Fig. S5, and their corresponding energetics are presented in Table S1 in the Supplemental Data. The lowest-energy conformer for each chemical structure was retained for comparison with the experiment. This comparison is shown in the lower panels of Fig. 4, giving evidence that the 2-carboxy-aziridine structure provides the closest match in the mid-IR. The compelling quality of this match is illustrated more clearly in Fig. S6 in the Supplemental Data, showing that the experimental band positions at 1767, 1529, 1417, 1159, 1009, 880, and 592 cm^{-1} are faithfully reproduced by the calculations. The two predicted bands in the hydrogen stretching region at 3412 and 3547 cm^{-1} also match with the observed peaks at 3414 and 3547 cm^{-1}; however, the predicted band at 3250 cm^{-1} is notably absent in the IRMPD spectrum. This absence could be attributed to several possible reasons. In general, lower-energy modes are often more difficult to observe (see, for example, the difference in intensity between the calculated IR spectrum for serine and the measured IRMPD spectrum for serine at ~3345 cm^{-1} in Fig. 3). Nonetheless, it is somewhat unexpected to see no (rather than a weak) peak. Thus it is possible that there is red-shifting of the band due to anharmonicity, which would not have been accounted for in harmonic frequency calculations and which may have moved the band outside of the measured region (*i.e.*, <3200 cm^{-1}). Incidentally, the spectrum measured here agrees with previous reports for product ion structures from protonated phosphoserine [20], which are expected to have the same ion structures as those proposed here.

In summary, this study provides compelling evidence that sulfoserine, like phosphoserine, likely produces a fragment ion with an aziridine structure as the dominant constituent of the *m*/*z* 88 ion, generated *via* loss of 98 amu from the modified side chain. As was reported previously for phosphoserine [20], it likely follows that the activation energy going to the lowest-energy structure (*i.e.*,

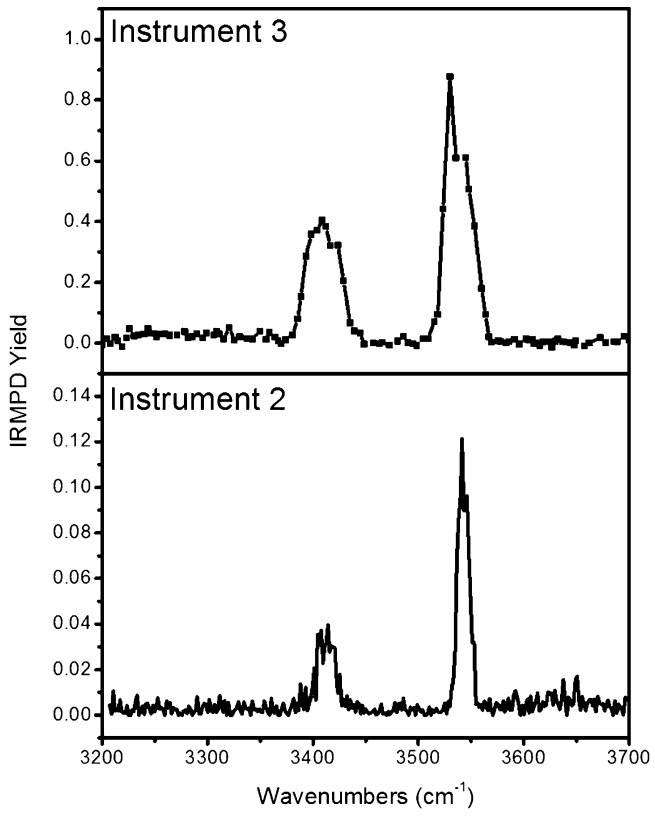

Fig. 5. Comparison of IRMPD spectra of the *m*/*z* 88 fragment ion recorded on two separate instruments to establish the reproducibility of these measurements between instruments and laboratories. The top spectrum was recorded on a custom QMF-QIT-ToF coupled to a cw OPO (described as instrument 3 in the experimental section of this paper), and the bottom spectrum was recorded on a modified Thermo LCQ instrument coupled to a pulsed OPO (described as instrument 2 in the experimental section of this paper).

2-amino-propenoic acid) is prohibitively high, allowing the higher-energy 2-carboxy-aziridine structure to be formed preferentially. In other words, the fragmentation process is kinetically, rather than thermodynamically, controlled.

3.3. Reproducibility

For any experimental technique, a demonstration of reproducibility is useful. As IRMPD spectroscopy is a qualitative technique, band positions and relative intensities are key markers of reproducibility. Since there are many experimental parameters (*e.g.*, laser intensity, ion cloud/IR beam overlap, type of mass spectrometer) which may differ from setup to setup, it is especially useful to determine inter-setup reproducibility. Thus, we have recorded the IRMPD spectrum of the *m*/*z* 88 fragment ion over the range of 3200–3700 cm^{-1} on two different instruments (described as instruments 2 and 3 in the experimental section of this paper) and present the results in Fig. 5. Though both the mass spectrometers and OPOs used to obtain these measurements are significantly different, the results also show many striking similarities, as one would hope. The absolute fragmentation yields and bandwidths were different due to differing experimental conditions, but the band positions and general shapes were reproduced with high fidelity. In addition, the relative intensities showed an enhanced yield for the 3547 cm^{-1} band over the 3414 cm^{-1} band. This supports the case for IRMPD spectroscopy as a robust analytical technique.

4. Conclusions

This work provides the first direct structural investigation of the fragmentation pathways of protonated sulfoserine at a fundamental level. Based on the evidence provided herein, several specific conclusions can be drawn about these fragmentation pathways:

- Upon CID, protonated sulfoserine undergoes fragmentation to give rise to four fragment ions at *m*/*z* 140, 129, 106, and 88. The fragment ions at *m*/*z* 106 and 88 are by far the most prevalent and correspond to the loss of the sulfate modification (as SO_3 and H_2SO_4, respectively).
- The fragment ion at *m*/*z* 106 is analogous to protonated serine, as evidenced by comparison to both synthetic serine and to calculated IR spectra.
- The major *m*/*z* 88 product ion adopts a 2-carboxy-aziridine structure.

This work presents one of the first attempts to understand the fragmentation chemistry of sulfoserine *via* spectroscopic means, laying the groundwork for future studies into the fragmentation chemistry of both larger sulfated systems (*e.g.*, peptides) and other (labile) biological modifications.

Conflict of interest

The authors declare no conflict of interest.

Acknowledgements

This research is financially supported by the National Science Foundation under grant CHE-1403262. AP acknowledges financial support from the University of Florida Graduate Student Fellowship and the National Science Foundation Graduate Research Fellowship under grant DGE-1315138. Furthermore, AP thanks the University of Florida Graduate Student Research Abroad Program for providing an award for travel to the Netherlands and France to conduct several of the experiments presented herein. The authors would like to thank the FELIX staff for skillful assistance, in particular Dr. Britta Redlich and Dr. Lex van der Meer. NCP acknowledges the NSF-PIRE grant (OISE-0730072) for travel support to the Netherlands.

Appendix A. Supplementary data

Supplementary data associated with this article can be found, in the online version, at http://dx.doi.org/10.1016/j.ijms.2014.12.001.

References

[1] D.A. Meh, K.R. Siebenlist, S.O. Brennan, T. Holyst, M.W. Mosesson, The amino acid sequence in fibrin responsible for high affinity thrombin binding, Thromb. Haemost. 85 (2001) 470–474.
[2] E. Skrzypczak-Jankun, V.E. Carperos, K.G. Ravichandran, A. Tulinsky, M. Westbrook, J.M. Maraganore, Structure of the hirugen and hirulog 1 complexes of α-thrombin, J. Mol. Biol. 221 (1991) 1379–1393.
[3] F.R. Bettelheim, Tyrosine-O-sulfate in a peptide from fibrinogen, J. Am. Chem. Soc. 76 (1954) 2838–2839.
[4] S. Costagliola, V. Panneels, M. Bonomi, J. Koch, M.C. Many, G. Smits, G. Vassart, Tyrosine sulfation is required for agonist recognition by glycoprotein hormone receptors, EMBO J. 21 (2002) 504–513.
[5] K.F. Medzihradszky, Z. Darula, E. Perlson, M. Fainzilber, R.J. Chalkley, H. Ball, D. Greenbaum, M. Bogyo, D.R. Tyson, R.A. Bradshaw, A.L. Burlingame, O-sulfonation of serine and threonine: mass spectrometric detection and characterization of a new posttranslational modification in diverse proteins throughout the eukaryotes, Mol. Cell. Proteomics 3 (2004) 429–440.
[6] C. Seibert, T.P. Sakmar, Toward a framework for sulfoproteomics: synthesis and characterization of sulfotyrosine-containing peptides, Pept. Sci. 90 (2008) 459–477.

[7] P.J. Boersema, S. Mohammed, A.J.R. Heck, Phosphopeptide fragmentation and analysis by mass spectrometry, J. Mass Spectrom. 44 (2009) 861–878.
[8] T.B. Schreiber, N. Mäusbacher, S.B. Breitkopf, K. Grundner-Culemann, H. Daub, Quantitative phosphoproteomics – an emerging key technology in signal-transduction research, Proteomics 8 (2008) 4416–4432.
[9] T.E. Thingholm, O.N. Jensen, M.R. Larsen, Analytical strategies for phosphoproteomics, Proteomics 9 (2009) 1451–1468.
[10] R.E. Bossio, A.G. Marshall, Baseline resolution of isobaric phosphorylated and sulfated peptides and nucleotides by electrospray ionization FTICR MS: another step toward mass spectrometry-based proteomics, Anal. Chem. 74 (2002) 1674–1679.
[11] A.L. Patrick, C.N. Stedwell, N.C. Polfer, Differentiating sulfopeptide and phosphopeptide ions via resonant infrared photodissociation, Anal. Chem. 86 (2014) 5547–5552.
[12] K.E. Hersberger, K. Håkansson, Characterization of O-sulfopeptides by negative ion mode tandem mass spectrometry: superior performance of negative ion electron capture dissociation, Anal. Chem. 84 (2012) 6370–6377.
[13] K.F. Medzihradszky, S. Guan, D.A. Maltby, A.L. Burlingame, Sulfopeptide fragmentation in electron-capture and electron-transfer dissociation, J. Am. Soc. Mass Spectrom. 18 (2007) 1617–1624.
[14] M.R. Robinson, K.L. Moore, J.S. Brodbelt, Direct identification of tyrosine sulfation by using ultraviolet photodissociation mass spectrometry, J. Am. Soc. Mass Spectrom. 25 (2014) 1461–1471.
[15] Y. Yu, A.J. Hoffhines, K.L. Moore, J.A. Leary, Determination of the sites of tyrosine O-sulfation in peptides and proteins, Nat. Methods 4 (2007) 583–588.
[16] N.C. Polfer, Infrared multiple photon dissociation spectroscopy of trapped ions, Chem. Soc. Rev. 40 (2011) 2211–2221.
[17] T.D. Fridgen, Infrared consequence spectroscopy of gaseous protonated and metal ion cationized complexes, Mass Spectrom. Rev. 28 (2009) 586–607.
[18] C.F. Correia, C. Clavaguera, U. Erlekam, D. Scuderi, G. Ohanessian, IRMPD spectroscopy of a protonated, phosphorylated dipeptide, ChemPhysChem 9 (2008) 2564–2573.
[19] F. Lanucara, B. Chiavarino, M.E. Crestoni, D. Scuderi, R.K. Sinha, P. Maître, S. Fornarini, S-nitrosation of cysteine as evidenced by IRMPD spectroscopy, Int. J. Mass Spectrom. 330–332 (2012) 160–167.
[20] F. Lanucara, B. Chiavarino, D. Scuderi, P. Maitre, S. Fornarini, M.E. Crestoni, Kinetic control in the CID-induced elimination of H_3PO_4 from phosphorylated serine probed using IRMPD spectroscopy, Chem. Commun. 50 (2014) 3845–3848.
[21] R.K. Sinha, B. Chiavarino, M.E. Crestoni, D. Scuderi, S. Fornarini, Tyrosine nitration as evidenced by IRMPD spectroscopy, Int. J. Mass Spectrom. 308 (2011) 209–216.
[22] B. Paizs, B. Bythell, P. Maître, Rearrangement pathways of the a_4 ion of protonated YGGFL characterized by IR spectroscopy and modeling, J. Am. Soc. Mass Spectrom. 23 (2012) 664–675.
[23] B.R. Perkins, J. Chamot-Rooke, S.H. Yoon, A.C. Gucinski, A.R.D. Somogyi, V.H. Wysocki, Evidence of diketopiperazine and oxazolone structures for HA b_2^+ ion, J. Am. Chem. Soc. 131 (2009) 17528–17529.
[24] M. Tirado, N.C. Polfer, Defying entropy: forming large head-to-tail macrocycles in the gas phase, Angew. Chem. 124 (2012) 6542–6544.
[25] J. Grzetic, J. Oomens, Spectroscopic evidence for an oxazolone structure in anionic b-type peptide fragments, J. Am. Soc. Mass Spectrom. 23 (2012) 290–300.
[26] A.M. Palumbo, G.E. Reid, Evaluation of gas-phase rearrangement and competing fragmentation reactions on protein phosphorylation site assignment using collision induced dissociation-MS/MS and MS^3, Anal. Chem. 80 (2008) 9735–9747.
[27] A.M. Palumbo, J.J. Tepe, G.E. Reid, Mechanistic insights into the multistage gas-phase fragmentation behavior of phosphoserine- and phosphothreonine-containing peptides, J. Proteome Res. 7 (2008) 771–779.
[28] G. Reid, R. Simpson, R.J. O'Hair, Leaving group and gas phase neighboring group effects in the side chain losses from protonated serine and its derivatives, J. Am. Soc. Mass Spectrom. 11 (2000) 1047–1060.
[29] D. Oepts, A.F.G. van der Meer, P.W. van Amersfoort, The Free-Electron-Laser user facility FELIX, Infrared Phys. Technol. 36 (1995) 297–308.
[30] J.J. Valle, J.R. Eyler, J. Oomens, D.T. Moore, A.F.G. van der Meer, G. von Helden, G. Meijer, C.L. Hendrickson, A.G. Marshall, G.T. Blakney, Free electron laser-Fourier transform ion cyclotron resonance mass spectrometry facility for obtaining infrared multiphoton dissociation spectra of gaseous ions, Rev. Sci. Instrum. 76 (2005) 023103.
[31] A.G. Marshall, T.C.L. Wang, T.L. Ricca, Tailored excitation for Fourier transform ion cyclotron mass spectrometry, J. Am. Chem. Soc. 107 (1985) 7893–7897.
[32] B. Schindler, J. Joshi, A.-R. Allouche, D. Simon, S. Chambert, V. Brites, M.-P. Gaigeot, I. Compagnon, Distinguishing isobaric phosphated and sulfated carbohydrates by coupling of mass spectrometry with gas phase vibrational spectroscopy, Phys. Chem. Chem. Phys. 16 (2014) 22131–22138.
[33] K. Gulyuz, C.N. Stedwell, D. Wang, N.C. Polfer, Hybrid quadrupole mass filter/quadrupole ion trap/time-of-flight-mass spectrometer for infrared multiple photon dissociation spectroscopy of mass-selected ions, Rev. Sci. Instrum. 82 (2011) 054101.
[34] A.-R. Allouche, Gabedit—a graphical user interface for computational chemistry softwares, J. Comput. Chem. 32 (2011) 174–182.
[35] M.J. Frisch, G.W. Trucks, H.B. Schlegel, G.E. Scuseria, M.A. Robb, J.R. Cheeseman, G. Scalmani, V. Barone, B. Mennucci, G.A. Petersson, H. Nakatsuji, M. Caricato, X. Li, H.P. Hratchian, A.F. Izmaylov, J. Bloino, G. Zheng, J.L. Sonnenberg, M. Hada, M. Ehara, K. Toyota, R. Fukuda, J. Hasegawa, M. Ishida, T. Nakajima, Y. Honda, O. Kitao, H. Nakai, T. Vreven, J.A. Montgomery Jr., J.E. Peralta, F. Ogliaro, M.J. Bearpark, J. Heyd, E.N. Brothers, K.N. Kudin, V.N. Staroverov, R. Kobayashi, J. Normand, K. Raghavachari, A.P. Rendell, J.C. Burant, S.S. Iyengar, J. Tomasi, M. Cossi, N. Rega, N.J. Millam, M. Klene, J.E. Knox, J.B. Cross, V. Bakken, C. Adamo, J. Jaramillo, R. Gomperts, R.E. Stratmann, O. Yazyev, A.J. Austin, R. Cammi, C. Pomelli, J.W. Ochterski, R.L. Martin, K. Morokuma, V.G. Zakrzewski, G.A. Voth, P. Salvador, J.J. Dannenberg, S. Dapprich, A.D. Daniels, Ö. Farkas, J.B. Foresman, J.V. Ortiz, J. Cioslowski, D.J. Fox, Gaussian 09, Revision A.2, Gaussian, Inc., Wallingford, CT, USA, 2009.
[36] C.J. Johnson, M.A. Johnson, Vibrational spectra and fragmentation pathways of size-selected, D_2-tagged ammonium/methylammonium bisulfate clusters, J. Phys. Chem. A 117 (2013) 13265–13274.
[37] M. Hanwell, D. Curtis, D. Lonie, T. Vandermeersch, E. Zurek, G. Hutchison, Avogadro: an advanced semantic chemical editor, visualization, and analysis platform, J. Cheminform. 4 (2012) 17.
[38] N.N. Dookeran, T. Yalcin, A.G. Harrison, Fragmentation reactions of protonated α-amino acids, J. Mass Spectrom. 31 (1996) 500–508.
[39] F. Rogalewicz, Y. Hoppilliard, G. Ohanessian, Fragmentation mechanisms of α-amino acids protonated under electrospray ionization: a collisional activation and ab initio theoretical study, Int. J. Mass Spectrom. 195–196 (2000) 565–590.
[40] M. Rožman, Modelling of the gas-phase phosphate group loss and rearrangement in phosphorylated peptides, J. Mass Spectrom. 46 (2011) 949–955.
[41] T. Yalcin, C. Khouw, I.G. Csizmadia, M.R. Peterson, A.G. Harrison, Why are B ions stable species in peptide spectra? J. Am. Soc. Mass Spectrom. 6 (1995) 1165–1174.
[42] W.D. van Dongen, W. Heerma, J. Haverkamp, C.G. de Koster, The diagnostic value of the m/z 102 peak in the positive-ion fast-atom bombardment mass spectra of peptides, Rapid Commun. Mass Spectrom. 9 (1995) 845–850.